PRELIMINARY DESIGN OF A HIGGS FACTORY $\mu^+\mu^-$ STORAGE RING[*]

A.V. Zlobin[#], Y.I. Alexahin, V.V. Kapin, V.V. Kashikhin, N.V. Mokhov, I.S. Tropin,
FNAL, Batavia, IL 60510, U.S.A.

Abstract

A Muon Collider (MC) offers unique possibilities for studying the recently found Higgs boson. However, there are difficulties specific to such a machine, most notably a very large aperture of superconducting (SC) magnets both in the Interaction Region (IR) and the rest of the Storage Ring (SR) due to a relatively large beam emittance as well as the necessity to protect magnets and detector from showers generated by muon decay products. A preliminary design and the first results of a complex approach to these problems for the 125 GeV c.o.m. Higgs Factory are presented which provides an average luminosity ~$2 \cdot 10^{31}$ cm^{-2}s^{-1} with a 4 MW proton driver.

INTRODUCTION

Recent observations of a relatively low mass Higgs boson boosted interest in a low-energy medium-luminosity $\mu^+\mu^-$ collider as a Higgs Factory (HF) [1]. In muon collisions the Higgs boson can be produced in reasonable amounts in the *s*-channel at the muon beam energy of just 62.5 GeV. Absence in MC of brems- and beam-strahlung (features limiting the performance of e^+e^- machines) makes possible a direct precision measurement of the Higgs boson mass and width. However, to obtain a sufficiently high luminosity with relatively large beam emittance quite small values of the beta-function (a few cm) at the Interaction Point (IP) are required resulting in a large beam size in the Final Focus (FF) quadrupoles. This factor, as well as the magnet and detector protection from the muon decay products, requires very large aperture of the IR magnets posing challenging engineering constraints and presenting beam dynamics issues with magnet fringe fields and the body field quality.

This paper describes a preliminary design of the Higgs Factory collider lattice and the IR layout as well as first results of simulations of heat deposition in SC magnets.

COLLIDER LATTICE

The HF Storage Ring parameters are shown in Table 1. A major requirement to the HF lattice is its ability to sustain a very low energy spread in the presence of strong self-fields. As a result, the IR chromaticity correction is still needed for compensation of the path-lengthening due to betatron oscillations. Furthermore, in contrast with a high-energy MC, a large momentum compaction factor ($\alpha_c \sim 0.1$) is required for the RF voltage to overcome self-fields without increasing the energy spread.

For chromaticity correction we use the 3-sextupole scheme developed for high energy MC [2]. It requires

Table 1: Higgs Factory Storage Ring Parameters

Parameter	Unit	Value
Beam energy	GeV	62.5
Transverse emittance, $\varepsilon_{\perp N}$	(π)mm·rad	0.3
Longitudinal emittance, $\varepsilon_{\parallel N}$	(π)mm·rad	1.0
Number of bunches/beam		1
Number of muons/bunch		2×10^{12}
Number of IPs		1
Circumference	m	300
Beam energy spread	%	0.003
Bunch length	cm	5.64
β^*	cm	2.5
Repetition rate	Hz	30
Proton driver power	MW	4
Average luminosity	cm^{-2}s^{-1}	2.5×10^{31}

high-field dipoles to be placed immediately after the FF multiplet. To reduce the dispersion invariant the horizontal beta-function at the dipole locations must be sufficiently small which means that the last quadrupole from the IP in the FF multiplet has to be defocusing.

The detector backgrounds can be reduced by a dipole component in the FF quadrupoles [2]. Since the horizontally bending field provides most efficient cleaning in defocusing quadrupoles it is preferable to make the Q2 defocusing. This leaves two options for the FF multiplet: a doublet [2] or a quadruplet. The latter is preferable since it allows reducing the magnet aperture.

The IR design assumes the 3.5 m distance of Q1 from the IP and a bore diameter of ($10\sigma_{max}+30$) mm. Figure 1 shows the 5σ beam envelopes and the required magnet inner radii. Table 2 shows the IR magnet parameters. Splitting Q2 in two parts allows for a mask in between.

The optics functions in half ring (starting from IP) are shown in Fig. 2 for $\beta^*=2.5$ cm. Note that with this IR design, β^* can be varied from 1.5 to 10 cm by changing the gradients in matching sections without perturbing the dispersion function. The momentum acceptance of the ring exceeds ±0.5%.
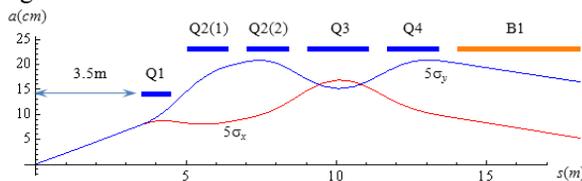

Figure 1: HF IR layout and beam size variations.

Table 2: IR Magnet Specifications

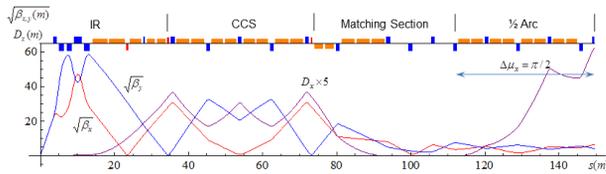| Parameter	Q1	Q2	Q3	Q4	B1
Aperture (mm)	270	450	450	450	450
Gradient (T/m)	74	-36	44	-25	0
Dipole field (T)	0	2	0	2	8
Magnetic length (m)	1.00	1.40	2.05	1.70	4.10

Figure 2: Layout and optics functions in half ring.

MAGNET DESIGNS AND PARAMETERS

Conceptual designs of the HF IR magnets are based on a 1 mm Nb_3Sn strand with J_c(12T,4.2K) of 2.7 kA/mm² and Cu/nonCu ratio of 1.15. The Q1-Q4 and B1 coils use a 42-strand Rutherford cable, 21.6 mm wide and 1.85 mm thick. The cable in the dipole coil B_q (in Q2 and Q4) has 22 strands and is 11.3 mm wide and 1.77 mm thick. Both cables are insulated with a 0.2 mm thick insulation.

The volume of all coils was chosen based on the operation margin and quench protection considerations. The coil aperture of IR magnets was increased by 50 mm to 320 mm in Q1 and to 500 mm in Q2-Q4 and B1 to provide adequate space for the beam pipe, helium channel and inner absorber (liner). The coil cross-sections were optimized with the ROXIE code [3] to achieve the required nominal gradient or field with sufficient operation margin and good field quality in the beam area.

The IR magnets use 6-layer, shell-type coils. The dipole coil B_q in Q2 and Q4 has only one layer. Q1 and Q2(1) do not have an iron yoke since they operate inside the detector field. Q2(2)-Q4 and B1 use the iron yoke mainly to reduce fringe fields. The optimized cross-sections of Q1-Q4 and B1 coils are shown in Fig. 3. The main magnet parameters at 4.5 K are reported in Table 3. The parameters for Q2 and Q4 (with dipole coil B_q) include the combined dipole and quadrupole fields. The B_q parameters include the field from the main quadrupole coil Q2 at G_{nom}=35 T/m. In Q4, the B_q parameters are better due to the lower G_{nom}=25 T/m.
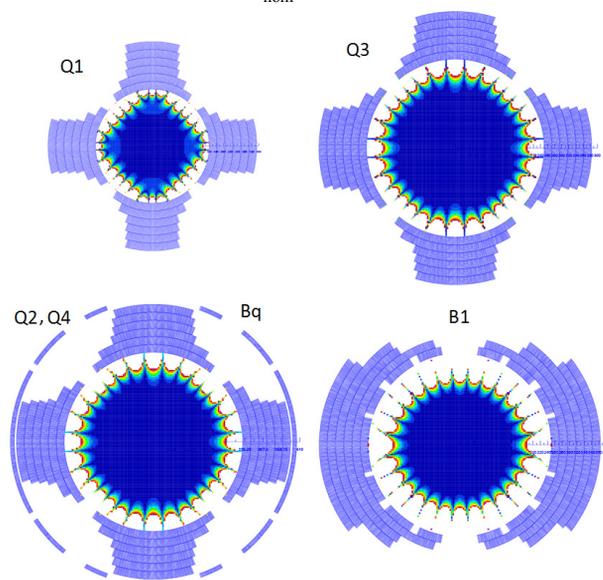

Figure 3: Coil cross-sections of IR magnets: Q1, Q3 (top), Q2 and Q4 with dipole coil B_q and B1 (bottom).

Table 3: IR Magnet Parameters at T_{op}=4.5 K

Parameter	Q1	Q2*	Q3	Q4*	Bq**	B1
Aperture (mm)	320	500	500	500	780	500
B_{max} (T)	-	-	-	-	4.18	16.3
G_{max} (T/m)	94.9	58.2	62.9	58.2	-	-
B_{t_max} coil (T)	16.4	17.2	16.9	17.2	15.0	17.7
Operation margin	0.78	0.62	0.70	0.62	0.48	0.50
L (mH/m)	177	454	454	454	65	1188
E_{op} (MJ/m)	10.4	11.3	16.8	5.5	1.6	13.8
$F_x(I_{op})$ (MN/m)	5.8	7.3	6.5	4.1	0.7	9.7
$F_y(I_{op})$ (MN/m)	-12.3	-12.6	-14.2	-6.8	-4.7	-8.9

* calculated for Bq_{nom}=2 T.
** calculated for G_{nom}=35 T/m (Q2).

The operation margin is defined as the ratio of magnet nominal to maximum field or field gradient. A 6-layer coil design provides sufficient operation margin in the IR magnets at relatively low current density in the coil. All the magnets operate at 50-80% of the short sample limit at 4.5 K. The quadrupole and dipole coils operate also at a high level of Lorentz forces. Stress management in the azimuthal direction will affect the coil efficiency and reduce the magnet operating margin. Conductor grading in the coil will provide additional margin if needed.

Geometrical field harmonics for Q1-Q4, B_q and B1 at corresponding R_{ref} are shown in Table 4. Coil cross-section optimization provided the relative field errors in the area occupied by muon beams on the level of 10^{-4} (dark blue area in Fig. 3). Analysis of the Dynamic Aperture (DA) with the MADX PTC code shows that field errors in the straight sections of the IR magnets reduce the DA by a factor of 2 so that it coincides with the good field region shown in Fig. 3.

Table 4: Geometrical Harmonics at R_{ref} (10^{-4})

Parameter	Q1	Q2-Q4	B_q	B1
R_{ref} (mm)	135	225	225	225
b_3	-	-	0.08	-0.07
b_5	-	-	0.05	-0.06
b_6	-0.56	-0.18	-	-
b_7	-	-	0.34	0.12
b_9	-	-	0.57	0.02
b_{10}	-0.47	-0.57	-	-
b_{11}	-	-	2.55	0.91
b_{13}	-	-	-2.89	1.58
b_{14}	3.45	-0.94	-	-

ENERGY DEPOSITION IN MAGNETS

For the HF parameters from Table 1, about 2.5×10^8 muon decays per bunch crossing produce extremely high fluxes of background particles in the collider detector. The decays from both beams result in a dynamic heat load in the Storage Ring of ~1 kW/m, i.e. ~300 kW total in the ring and IR magnets. This places exceptional constraints on the HF magnet design and their protection [2, 4].

Energy deposition and detector backgrounds are simulated with the MARS15 code [5]. All the related details of geometry, materials and magnetic fields are implemented in the model. As a major element of MDI
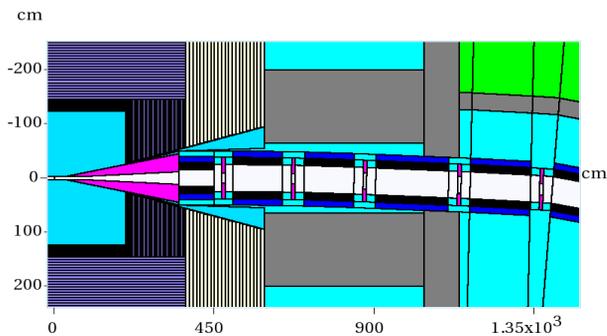
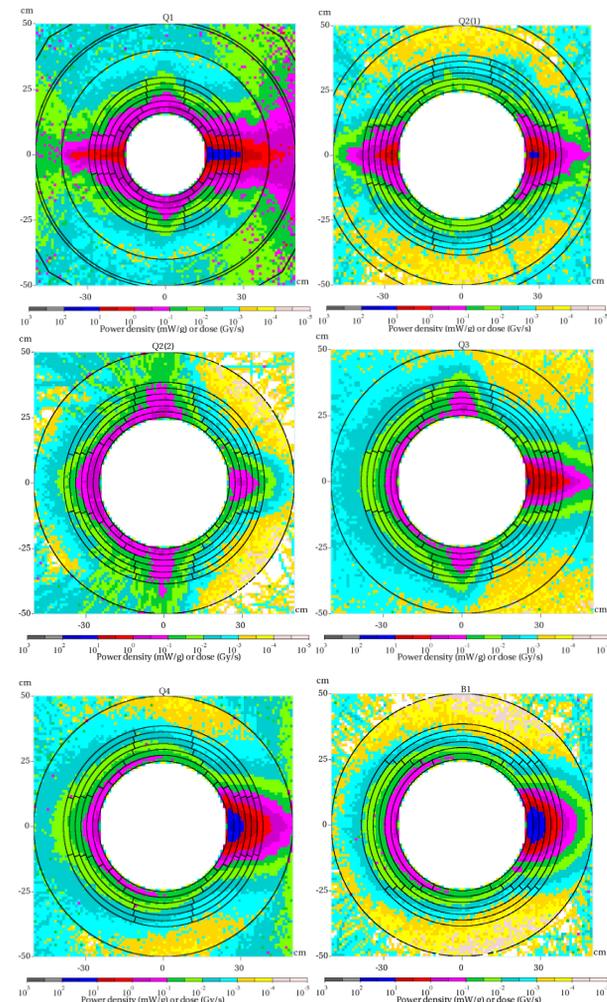Figure 4: MDI details in the MARS model (V1).

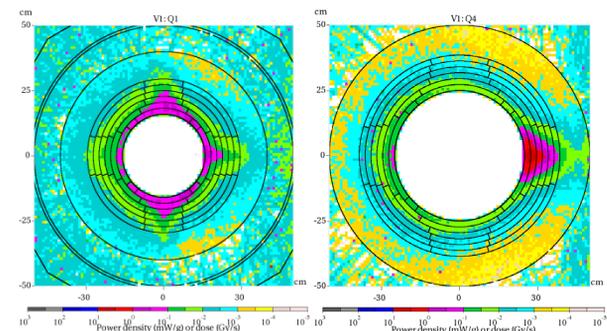Figure 5: Power density (mW/g) in IRQ and B1 (V0).

Figure 6: Power density (mW/g) in Q1 and Q4 (V1).

[2, 4], a tungsten nozzle with 5σ radius aperture was implemented in the model.

To protect IR magnets 10 cm long, 5σ radius aperture tungsten masks were realized in the interconnect regions. Two cases were simulated: a) without the masks (V0); and b) with the masks and concrete shielding around the FF quadrupoles in the MDI region (V1) (see Fig. 4).

The calculated distributions of power density in the Q1-Q4 quadrupoles and the B1 dipole are shown in Fig. 5. The maximum values of power density in the IR quadrupoles and first dipole are summarized in Table 5. In version V0, these numbers substantially exceed the quench limit for Nb_3Sn coils of ~5 mW/g [6].

Table 5: Peak power density (mW/g) in IR magnets.

	Q1	Q2(1)	Q2(2)	Q3	Q4	B1
V0	50	20	0.8	10	45	45
V1	0.8	7	0.6	0.7	9	30

Figure 6 and Table 5 demonstrate that the tungsten masks reduce the peak power density in Q1 and Q3 to 0.7-0.8 mW/g, i.e., below the coil quench limit with a good safety margin. In other IR magnets, the reduction is gradually less. Further mask optimization is underway. Moreover, there is a room for elliptical liners to further reduce peak power in the horizontal direction in Q2(1), Q4 and B1.

SUMMARY & OUTLOOK

Preliminary design and analysis of a Higgs Factory based on a low-energy $\mu+\mu-$ collider, including beam dynamics, magnet design concepts and radiation problems in IR magnets, have demonstrated the feasibility of such a machine and identified its limitations. Further studies will focus on:

a) the effect of 3D fringe fields on the dynamic aperture and its correction, the longitudinal dynamics with wake-fields and the beam-beam effect, and lattice optimization for higher quadrupole gradient;

b) magnet design optimization including 3D end fields, mechanics and quench protection;

c) optimization of the nozzle outer angle (requires changes to detector), the further optimization of IR collimators and MDI configuration, and the HF detector response simulations with the MARS-generated source.

REFERENCES

[1] https://hepconf.physics.ucla.edu/higgs2013/

[2] Y.I. Alexahin et al., "Muon Collider Interaction Region Design", PRSTAB, 14, 061001 (2011).

[3] ROXIE, http://cern.ch/roxie.

[4] N.V. Mokhov et al., "Muon Collider Interaction Region and Machine-Detector Interface Design", *Proc. of PAC2011*, NYC, March 2011, p. 82.

[5] MARS15, http://ww-ap.fnal.gov/MARS/.

[6] A.V. Zlobin et al., "Large-Aperture Nb_3Sn Quadrupoles for 2nd Generation LHC IRs", *Proc. of EPAC2002*, Paris, June 2002, p. 2451.